Crystallographic Analysis of the Inhibition of Porcine Pancreatic Elastase by a Peptidyl Boronic Acid: Structure of a Reaction Intermediate†,‡

Lori H. Takahashi,§ R. Radhakrishnan,∥ Richard E. Rosenfield, Jr.,∥ and Edgar F. Meyer, Jr.*,∥

Department of Chemistry and Department of Biochemistry and Biophysics, Texas A&M University, College Station, Texas 77843

Received February 6, 1989; Revised Manuscript Received April 21, 1989

ABSTRACT: The crystal structure of porcine pancreatic elastase (PPE) complexed to carbobenzoxy-alanylisoleucine-boronic acid (ZAIB) is reported to 2.09-Å resolution and refined to an *R* factor of 0.15. This is the first reported structural analysis of PPE with an isoleucine residue in the primary specificity pocket. The results include (1) marked displacement of the inhibitor *out* of the active site leading to (2) a close (2.2 Å) direct contact between B (boron atom of the inhibitor) and N_ϵ of His-57 and also (3) covalent bonding (1.5 Å) to O_γ of Ser-195. A scheme for the mechanism of inhibition of PPE by ZAIB is proposed. A comparison with a peptidyl difluoromethyl ketone-PPE complex (K_i = 9.5 μM) is made to explain the strong inhibition of PPE by ZAIB (K_i = 0.3 μM). These results lead us to characterize this structure as a time- and space-averaged reaction intermediate, providing fresh insight into the cramped dimensions available in enzymatic catalyses.

Elastases (EC 3.4.21.11) are believed to be the causative agent in the destructive diseases pancreatitis, emphysema, and rheumatoid arthritis. Most of the structural studies on elastases have concentrated on porcine pancreatic elastase (PPE)[1] due to the availability of a high-resolution (1.65 Å) native structure (Meyer et al., 1987) as well as the relative ease of cocrystallyzing with small molecule ligands. In addition, the complex of human leukocyte elastase (HLE) with turkey ovomucoid inhibitor third domain has recently been solved (Bode et al., 1986) to 1.7 Å, and the close structural homology at the active site between HLE and PPE has been discussed (Meyer & Bode, 1987). These relationships are the subject of a recent review (Bode et al., 1989).

It has long been believed that PPE prefers only small unbranched, nonpolar amino acids such as alanine in the S_1 [nomenclature of Schechter and Berger (1967)] subsite due to the marked constriction of the binding pocket by the side chains of Val-216 and Thr-226, which replace the corresponding Gly residues of trypsin and chymotrypsin. Studies with amides (Thompson & Blout, 1973), peptide 4-nitroanilides (Zimmerman & Ashe, 1977), and methyl esters (Geneste & Bender, 1969) have shown a preference for alanine at the P_1 position. However, studies with thiobenzyl ester substrates (Harper et al., 1984) show that isoleucine at P_1 gives rise to a stronger inhibition with PPE, with a K_m value 13 times lower than that of the corresponding alanine substrate. Recently, boronic acids with alanine, valine, and isoleucine at P_1 were examined as inhibitors of elastase (Kinder & Katzenellenbogen, 1985). It was found that isoleucine was a much better inhibitor than the valine analogue and was 350 times better than the alanine inhibitor. No structural data were available to suggest a reason for this preference, thus justifying this analysis.

Stein has investigated the P_1 specificity of HLE and has stated that the specificity is dependent on substrate length, becoming broader with decreasing chain length (Stein, 1985). He suggested that the relative rates of bond cleavage by larger elastase peptide substrates can differ significantly from those observed for the small substrates investigated. Powers and Gupton (1977) showed in the case of PPE that the relative probability of proteolysis was higher for larger peptides with P_1 residue isoleucine than for those with P_1 residue alanine (the ratio being 1:0.83).

Model building has shown that the side chains of methionine, leucine, and isoleucine can be accommodated in PPE's binding pocket (Papamokos et al., 1982). This relates directly to the reactive portion of the natural inhibitor α_1 proteinase inhibitor (Travis & Salvensen, 1983), where a Met-358 residue is found at P_1. However, the branched side chain at C_β in Ile adds an extra degree of difficulty or uncertainty to such modeling studies.

Boronic acids have been shown to be excellent inhibitors of PPE (Kettner & Shenvi, 1984; Kinder & Katzenellenbogen, 1985). The mode of inhibition is believed to be due to formation of a hemiacetal-like intermediate with the catalytic serine O_γ of the enzyme, resembling the tetrahedral intermediate postulated to be on the pathway for substrate hydrolysis.

To demonstrate the binding of a peptidyl boronic acid inhibitor with PPE and also the binding of a large, branched amino acid residue in the S_1 subsite, we undertook the crystal structure analysis of the complex of PPE with carbobenzoxy-Ala-Ile-boronic acid. A recent crystal structure of a peptidyl boronic acid complexed with α-lytic protease (Bone et al., 1987) reported covalent linkage of the boron atom of the inhibitor to the Ser-195 but not to His-57. Our analysis

† This work was supported by the Robert A. Welch Foundation (A-328), the Office of Naval Research, the Council for Tobacco Research-USA, and the Texas Agricultural Experiment Station.

‡ The atomic coordinates in this paper have been submitted to the Brookhaven Data Bank under the label 5EST.

* To whom correspondence should be addressed.

§ Department of Chemistry.

∥ Department of Biochemistry and Biophysics.

[1] Abbreviations: PPE, porcine pancreatic elastase; HLE, human leucocyte elastase; CBZ, carbobenzoxy; ILB, isoleucylboronic acid; NMR, nuclear magnetic resonance; BBA, benzeneboronic acid; ZAIB, CBZ-Ala-ILB; RMS, root mean square.

0006-2960/89/0428-7610$01.50/0

goes one step further, showing the boronic acid inhibitor to be doubly attached to the enzyme. Bone et al. (1989) now have studied boronic acids with Ala, Val, Ile, Nle, and Phe at the P_1 position. They report "what appears to be a coordinate covalent bond to boron" for the boro-Phe complex, similar to the structure reported here. However, their boro-Ile complex does not show a direct N–B contact (3.5 Å). These comparisons suggest rather interesting structure–function relationships that deserve further study.

Crystallization and Data Collection

The experiment was performed two times. The first time, the data were collected to 2.5-Å resolution. Because the resolution was held to be insufficient, we were asked to repeat the experiment with higher resolution data. Hence the second data were collected. Both the methods of crystallization and the data collection were completely different; however, the refinement and results remain the same in both the studies.

Crystal 1 (Diffusion Method). Commercially available PPE (Fluka 45125) was used without further purification. The inhibitor, Cbz-Ala-Ile-boronic acid (ZAIB), was synthesized and kindly supplied by Prof. John Katzenellenbogen of the University of Illinois. Crystals of PPE were grown from a 1.4% (w/v) solution of PPE in 0.1 M sodium phosphate and 0.1 M sodium sulfate (pH 5.0) by vapor diffusion. Two crystals were used for data collection. The crystals (size 0.35 × 0.20 × 0.15 mm and 0.30 × 0.35 × 0.35 mm) were soaked in the inhibitor solution for 24 h before being mounted in capillaries in contact with a small amount of inhibitor solution; data collection began ca. 30 days later, due to intervening experimental difficulties. The crystals crystallized in the space group $P2_12_12_1$ with cell constants of 51.78, 57.80, and 75.43 Å.

Data Collection. Diffraction data were collected at 25 °C on an automated Syntex-Datex four-circle diffractometer using an Enraf-Nonius generator operating at 40 kV and 26 mA, with a crystal to counter distance of 415 mm (helium tube). Ni-filtered Cu Kα radiation was used. Intensities were measured by 1° ω scans. Background intensities on both sides of the scans were measured, and six standard reflections were monitored periodically. Multiple scans of each reflection were made for reflections greater than 3σ and less than 10σ, where σ was determined from counting statistics. Intensities were corrected for Lorentz and polarization effects. No correction was made for absorption, and none was necessary for decay (less than 5%).

Data processing (scaling, merging, structure factor, and electron density calculations) was performed by using the PROTEIN (Steigemann, 1974) system of programs. A total of 7318 unique reflections was obtained, corresponding to 87% of the data to 2.53-Å resolution. The final R_{merge} (defined as $\sum(I_i - \langle I \rangle)/\sum I_i$, where I_i is the intensity value of an individual measurement, $\langle I \rangle$ is the corresponding mean value, and the summation is over all reflections common to two or more data sets) value ranged from 0.06 to 0.12, and the R_{symm} values ranged from 0.05 to 0.013.

Crystal 2 (Cocrystallization). The PPE and the inhibitor were allowed to react in 0.1 M sodium phosphate buffer at pH 5.0 with 20% methanol. The ratio of the molarity of inhibitor to that of the enzyme was 4:1. The concentration of the enzyme was 1.3% (w/v). The crystals of the inhibited enzyme were then obtained over 3 weeks by vapor diffusion from 0.1 M sodium phosphate and 0.1 M sodium sulfate and allowed to sit for 1 month. One crystal with dimensions 0.40 × 0.30 × 0.30 mm was used for data collection. The space group was $P2_12_12_1$, and the cell constants for this crystal were 52.28, 57.56, and 75.41 Å.

Data Collection. The crystal was placed on a FAST area detector and aligned along the needle (*b*) axis. Ni-filtered Cu Kα radiation from a Rigaku Ru 200 generator with fine-focus target (120 kV, 60 mA) was used, and the temperature was maintained at 5.5 °C. The asymmetric region of reciprocal space (−2.5° to 92.5°) was scanned at a rate of 120 s/0.1° step by using the MADNES system (Messerschmidt & Pflugrath, 1987), which also refined the crystal to detector distance (52 mm) and various crystal and camera parameters. Crystal missetting angles were refined every 5°. Subsequently, the crystal was rotated 30° about the χ axis, and an additional scan (−2.5 to 22.5°) was made. The data were scaled, corrected for absorption, and merged by using the program of Huber and Schneider (personal communication). Data were collected up to 2.0-Å resolution. A total of 19 661 reflections were collected, of which 11 021 reflections were unique and 10 569 reflections were treated as observed. The data are 73% complete to 2.09-Å resolution. The R_{merge} value was 3.9%. The entire data collection procedure required less than 4 days. Previous diffractometer measurements of repeat reflections showed less than 5% decay over 7 days; thus, no correction was indicated for crystal decay in this study.

Crystallographic Modeling and Refinement

An unbiased difference Fourier map ($F_o - F_c$) was calculated by using the phases and amplitudes from native porcine pancreatic elastase (Meyer et al., 1987) with all the solvent molecules as well as the Ser-195 and the His-57 removed. Removal of the latter residues was to determine in an unbiased way whether there was any covalent attachment between the enzyme and the inhibitor; this also serves as an independent check of the quality of the difference Fourier map. This map clearly showed the binding locus and orientation of the complex; alternative binding modes were therefore excluded.

In both studies, the initial difference Fourier map ($F_o - F_c$) showed a continuous Ser-195 O_γ to boron atom connection, and the density at the 2σ contour level was completely absent for one of the two hydroxyl oxygen atoms attached to the boron atom. For the first data set, the density for the bond connecting boron and the C_α carbon atom of the isoleucine residue in the inhibitor was absent; however, continuous residual density between His-57 and the B atom of the inhibitor was observed. In the case of the second data set, the residual density for the histidine side chain was very close to the density from the B atom of the inhibitor. In both cases, density for one of the hydroxyl oxygen atoms attached to the boron atom was clearly missing. These observations prompted us to conclude that a strong interaction exists between His-57 and the B atom. Density was present for the other boron hydroxyl oxygen atom; however, it was not located in the oxyanion hole, but pointed out toward solution. The final difference Fourier map is shown (Figure 1), with the contributions to F_c from Ser-195, His-57, and the inhibitor omitted. Because of the superiority of the data from crystal 2, the following discussions will refer only to these data, unless otherwise noted.

Initial coordinates for the inhibitor model were generated by using standard bond lengths, bond angles, and dihedral angles. The inhibitor was treated as a continuous chain bonded to Ser-195 O_γ. The putative coordinate covalent bond between the inhibitor boron atom and the His-57 N_ϵ was defined in the program EREF (Jack & Levitt, 1978; Deisenhofer et al., 1985) in the same way as a disulfide bond would be defined. An average of the covalent distance and the nonbonded distance was used for this approximate coordinate covalent bond (2.0 Å). However, a very low force constant (typically 10% of the covalent bond) was used so that the position of the atoms would

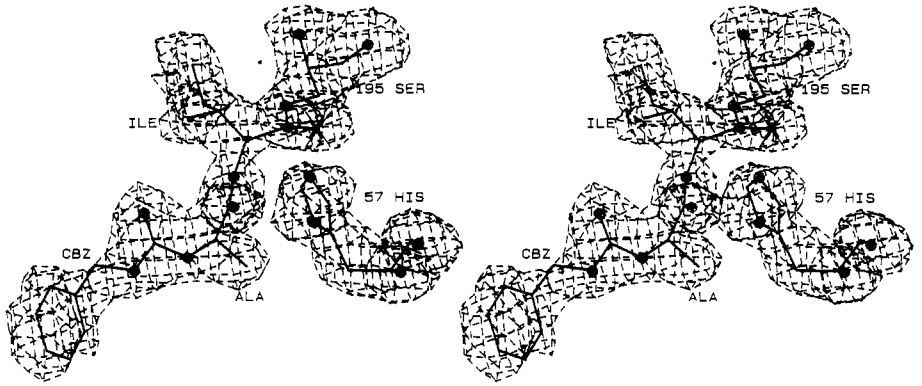

FIGURE 1: With the contributions (F_c) from the inhibitor, Ser-195, and His-57 removed, the final difference Fourier ($F_o - F_c$) map is drawn in stereo at 1.4σ (0.2 e/Å^3) density level. The inhibitor, His-57, and Ser-195 are drawn superimposed on the residual density. Continuous density between the inhibitor and Ser-195 is observed, as is the close approach of His-57 to the B atom. Only one OH group (marked with X) is seen attached to the B atom.

Table I: Final Parameters for the Cbz-Ala-Ile-Boronic Acid–PPE Complex Using Data from Crystal 2

R factor = $(\sum\|\|F_o\| - \|F_c\|\|/\sum\|F_o\|)$	0.15
resolution range (Å)	7–2.09
no. of reflections	10380
no. of atoms	2036
overall temp factor for complex (Å^2)	17.8
overall temp factor for inhibitor (Å^2)	18.0
SD for bond length (Å)	0.017
SD for bond angle (deg)	2.4
min and max cutoff for temp factor (Å^2)	4.0 and 50.0
min and max electron density in final ΔF map (e/Å^3)	−0.4 and 0.28
mean positional error (Luzzatti, 1952) (Å)	0.19
effective resolution (Swanson, 1988) (Å)	2.2

be more strongly dictated by the crystallographic densities.[2] The angles involved were treated as the average of trigonal and tetragonal angles, but with low weights. Likewise, the optimum values for the angles between the His-57 N_ϵ, boron, and the atoms attached to the boron (C and O) were given a value of 92° together with low weights. The scattering factors of Forsyth and Wells (1959) were used in the refinement, which was performed as described earlier (Meyer et al., 1986). In total, 202 water molecules were found. Refinement was terminated after 328 cycles with an R factor of 0.15. Other than the inhibitor complex (Figure 1), no other residual density above 0.25 e/Å^3 was observed in the map at structurally significant locations. The sulfate and calcium ions were located in their conserved locations. The enzyme–inhibitor complex final parameters are summarized in Table I and the geometric and refinement parameters in Table II.

[2] A referee has questioned the validity of our refinement procedure and its ability to establish the nature of the B–N contact. Two additional refinement procedures were therefore followed: (1) a "weak" force constant (5, cf. Table II) with a target bond length of 2.2 Å and (2) as nonbonded atoms with no designated force constant. The original refinement (2.0-Å target distance, weight 20% of a B–O bond) is described in Table II. Procedure 1 resulted in a refined B–N distance of 2.16 Å (overall standard deviation of bond lengths was 0.016 Å, R factor = 0.149), while the unconstrained refinement of procedure 2 resulted in a final B–N distance of 2.55 Å (overall standard deviation of bond lengths was 0.017 Å, R factor = 0.150). Because protein structures are so weakly underdetermined (10 380 measurements for over 3 times 2036 variables = 1.7), an unconstrained value cannot be taken as definitive. Indeed, the electron density dictates the bounded locus of atoms or groups of atoms. The two procedures collectively confirm the 2.2-Å B–N distance and subsequent assignment as a "coordinate coordinate bond". The resulting geometry is consistent with the observations of Bürgi et al. (1973) in that a slight puckering of the B atom toward the His-57 N_ϵ atom is observed, although it was not specified as the target model.

Table II: Optimum Values and the Refined Values for Some of the Parameters Involving the Boron Atom[a]

parameter	optimum	refined model	weight given
B···OH	1.36	1.38	100.0
B···O_γ	1.45	1.46	100.0
B···C_α	1.75	1.74	80.0
B···$N_{\epsilon 2}$	2.0	2.2	20.0
C_α–B–O_γ	118.0	115.2	30.0
C_α–B–OH	118.0	118.3	30.0
O_γ–B–OH	118.0	117.0	30.0
C_α–B–N	92.0	105.7	10.0
O_γ–B–N	92.0	97.5	10.0
OH–B–N	92.0	97.5	10.0
B–N–C_α	120.0	126.0	30.0

[a] The distances are in angstroms, and the angles are in degrees.

Description and Discussion

Our initial results (crystal 1, obtained in 1987) were unprecedented, and the analysis of crystal 2 (performed in 1988) gave identical results. It is therefore useful to consider previous studies with boronic acid inhibitors in an effort to understand the N–B "bond".

Organoboron compounds can exist in two general configurations. In one, the boron atom is trigonal coplanar with sp^2 hybridization having empty 2p orbitals. The boron atom is electron deficient in this state and capable of acquiring a fourth ligand to become tetrahedral with sp^3 hybridization.

The mechanism of boronic acid inhibition of serine proteases has been much discussed. The debate has focused on the identification of the reacting nucleophile (Ser or His) and the coordination number of the inhibited boron atom. Berezin and co-workers (Antonov et al., 1970) were the first to suggest the involvement of His-57 in the mechanism of inhibition of the boronic acids with serine proteases. In their studies of chymotrypsin with boric acid and *n*-alkylboronic acids, they found that inhibition was pH dependent.

Phillip and Bender (1971) also proposed imidazole complexation of benzeneboronic acid (BBA) with subtilisin from their studies on pH dependence, Hammett plots, and NMR studies. Inhibition was shown to be dependent upon two pK values, one near the pK_a of His-57 (pH 7) and the other at various pH values above 7. The second pK varied with the different boronic acid substrates used, which would correspond to the ionization of one of the boronic acid hydroxyl groups. Chemical shifts in boron-11 NMR studies were associated with trigonal to tetrahedral conversion of the boron atom upon complexation.

Temperature jump studies on boronic acids with subtilisin and chymotrypsin (Nakatani et al., 1975a,b) showed a two-step

mechanism involving a fast bimolecular association followed by a slow, unimolecular process.

$$E + S \underset{k_{-1}}{\overset{k_1}{\rightleftharpoons}} ES \underset{k_{-2}}{\overset{k_2}{\rightleftharpoons}} ES^*$$

In their studies, the step at which proton release occurred corresponded to the formation of the ES complex, because the values of k_1 increased monotonically with increasing pH, whereas the values of k_2/k_{-2} decreased. The ratio k_2/k_{-2} represents the ratio of ES to ES* at each pH. From the pH dependence of the inhibitor constant of BBA the amino acid residue responsible for proton release was determined to be His-57. The pH dependence of k_1 also suggested that the deprotonated form of histidine was binding with BBA. Even upon binding with BBA in the neutral or acidic region, the protonation equilibrium of His-57 of the enzyme was shifted toward the deprotonation state. This equilibrium shift leads to overall proton release from the system. In the D_2O studies of Nakatani (1975b), proton transfer was found to be involved in the ES to ES* conversion.

Two explanations for the process could be given: the first is a conformational change of the enzyme going from ES to ES*; the other is trigonal to tetrahedral interconversion at the active site. The values for k_2 and k_{-2} were comparable in magnitude to acylation or deacylation processes which range from 10^1 to 10^3 s^{-1}. Thus, it was concluded that the inhibitor was undergoing trigonal to tetrahedral conversion. Berry and co-workers (Berry et al., 1988) have used circular dichroism studies to suggest that the second-phase ES–ES* does not involve any major conformational change.

Lindquist and Terry (1974) suggested the development of a negatively charged tetrahedral adduct between boronic acids and the catalytic serine of subtilisin Carlsberg. These conclusions were derived from pH studies and knowledge of the crystallographic study on subtilisin inhibition by boronic acids (Kraut, 1977). The NMR studies of Robillard and Schulman (1974) also supported the presence of negatively charged adducts of the boronic acid. B–N bonding has been reported from NMR experiments by Bachovchin et al. (1988); however, their report of two distinct states (type 1 and type 2) is at variance with the crystallographic result reported here. One would have to look at α-lytic protease complexes for more direct support of their report.

Evidence against the involvement of catalytic histidine in attacking the boron atom of the inhibitor as a nucleophile was presented when the 2.5-Å crystal structure of subtilisin BPN′ with BBA and (2-phenylethyl)boronic acid was originally solved (Matthews et al., 1975). The catalytic serine O_γ (Ser-221, in this case) formed a covalent bond with the boron atom of the inhibitor, which was described as being tetrahedral. One of the hydroxyl groups was located in the oxyanion hole, defined in subtilisin by the amido nitrogen atom of Ser-221 and the side-chain NH_2 group of Asn-115. The second hydroxyl group was within hydrogen-bonding distance to the N_ϵ of the catalytic histidine (His-64) (2.8 Å), but the angle at the hydrogen atom was poor. It was also mentioned that the density for this oxygen atom was weak, but they concluded it was due to the disordering of solvent.

With (2-phenylethyl)boronic acid (Matthews et al., 1975), two binding modes were found. One was analogous to that of BBA, but in the second binding mode, the phenylethyl side chain was located near the S_1' subsite; the hydrogen bonds to the oxyanion hole or His-64 were not formed, and no covalent bond was formed between Ser-221 and the boron atom.

In another instance, the boronic acid complex with the elastase-like α-lytic protease (Bone et al., 1987) also shows no B–His bond. The catalytic serine O_γ formed a covalent bond with the boron atom of the inhibitor, which was described as being oriented tetrahedrally even though the geometry at the boron atom tended to be more trigonal after refinement, with the serine O_γ to boron distance of 1.68 Å.

The crystal structure of the boronic acid inhibitor with PPE is strikingly different from the boronic acid complex with subtilisin discussed above. His-57 is identically positioned (χ_1 here 80°, in native PPE 79°), and thus the boron atom locates itself to let the N_ϵ of His-57 make a coordinate covalent bond (2.2 Å) with it. This rather long B–N distance restrains us from denoting this as a formal coordinate covalent bond. Moeckli et al. (1988) interpret the existence of a long B–N distance in terms of a dative bond between lone-pair electrons on the N atom and an empty $2p_z$ orbital on B. The close proximity of the His-57 N_ϵ atom excludes the possibility of the other hydroxyl oxygen atom being present, as supported by the difference Fourier maps from both the data sets. At pH 5.0 the histidine is more likely to be protonated and thus capable of donating a hydrogen atom to one of the boron hydroxyl oxygen atoms followed by concomitant loss of water. This would explain the unambiguous absence of density for one of the boron hydroxyl groups.

Tsai and Bender (1984) found a pH dependence of binding of BBA to PPE with two pK values. They concluded that serine played an essential role in the inhibition by conducting similar studies using anhydroelastase, with its active-site Ser $O_\gamma H$ removed. They compared an aldehyde inhibitor in which the K_i went from 8×10^{-7} to values in the range 10^{-3}–10^{-2} with the boronic acid inhibitor in which the K_i went from 1.6×10^{-3} to ca. 4.5×10^{-2}. The magnitude of the differences in K_i values suggests that serine is playing a significant role in inhibition, but it does not preclude the activity of histidine as a nucleophile.

The following reaction occurs at a pH above 7.5:

$$R\text{–}B(OH)_2 + OH^- \rightarrow R\text{–}B(OH)_3^-$$

Because this study was performed at pH 5.0, it is assumed that Ser-195 is attacking a trigonal boron atom. The inclusion of histidine in the mechanism seems likely, due to the fact that these inhibitors exhibit slow-binding kinetics. Kettner and Shenvi (1984) have seen that a relatively weak EI complex is formed initially (K_i = 18–30 nM) but then undergoes a slow conversion to a more tightly bound complex (K_i = 0.2–0.3 nM). The slow conversion could be due to the trigonal to tetrahedral conversion as was believed, but one should see a deuterium isotope effect on k_2, as in the study of Nakatani (1975b). However, in this case, it was not seen. Due to the absence of a definitive deuterium isotope effect and the high affinity of these compounds versus the aldehydes (e.g., chymostatin with chymotrypsin had a K_i of 10^{-7}, but the boronic acid K_i was ca. 10^{-10}), Kettner and Shenvi concluded that a major conformational change in the enzyme is taking place. Both the aldehydes and boronic acids may be considered to be transition-state analogue inhibitors; however, the aldehyde Ac-Pro-Ala-Pro-alaninal with PPE had a K_i of 2 μM (Thompson & Blout, 1973), while the boronic acid Suc-Ala-Ala-Pro-Ala-B(OH)$_2$ had a K_i of 3×10^{-10} M (Kettner & Shenvi, 1984). Because both inhibitors form tetrahedral intermediates with the enzyme, we conclude that the difference in binding constants is due to electron-pair donation by the unprotonated N_ϵ atom of His-57. The related structural analysis of a peptidyl boronic acid complex with α-lytic protease (Bone et al., 1987) shows covalent attachment of the boron atom to Ser-195 but not to His-57. This difference between the two structures may be directly attributed to the

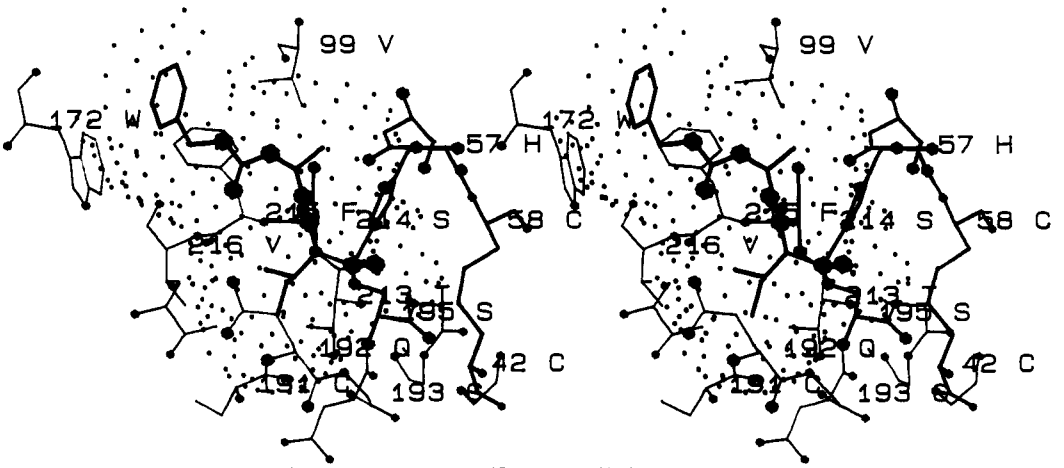

FIGURE 2: Interface contact surface generated by program FRODO (Jones, 1978) drawn in stereo, showing the title complex in the active site of PPE. Heteroatoms are drawn as spheres by using the BLOB option (Karrer, unpublished program). His-57 is shown "bound" to the B atom; it retains its hydrogen-bonding location, characteristic of the catalytic tetrad in native PPE.

Scheme I: Inhibition of PPE by ZAIB[a]

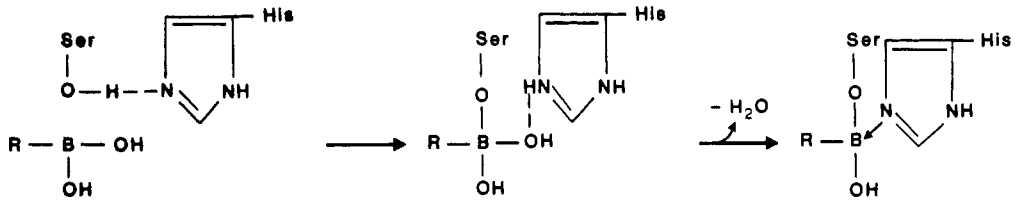

[a] (a) The inhibitor and the enzyme supposedly form a Michaelis complex. (b) The boron atom of the inhibitor is attacked by the O_γ atom of the active-site Ser-195. The His-57 N_ϵ is very close to one of the O atoms attached to the B atom. (c) His-57 donates the proton to the hydroxyl oxygen atom, producing a water molecule, and the His-57 N_ϵ atom makes a coordinate covalent bond with the boron atom.

"poor" insertion of Ile into the S_1 pocket of PPE, causing a dramatic outward displacement of the inhibitor, thus providing a favorable contact distance for His-57 attack. The steric bulk and "lock and key" fit of the boronic acid inhibitor is illustrated (Figure 2).

We propose the mechanism for the inhibition of PPE by Cbz-Ala-Ile boronic acid shown in Scheme I. The mechanism first involves the nucleophilic attack on the boron atom by Ser-195 O_γ to give a tetrahedral boron–enzyme adduct. This is followed by His-57 donating a proton to the nearby hydroxyl group followed by loss of water to give a trigonal boron complex (which resembles the acyl enzyme). The release of the hydroxyl group from the inhibitor boron atom seems to be the step responsible for distinguishing the second K_i in the time scale found in the case of boronic acids. Next, His-57 N_ϵ tries to form a coordinate covalent bond with boron. This part of the reaction is not yet complete in the present structure due to a compromising situation attributed to the fact that the His-57 N_ϵ is tied to the backbone of the protein on one hand and the boron atom itself is covalently bound to the serine on the other hand. These factors would therefore balance and likewise limit how far these two atoms can approach in forming a formal coordinate covalent bond.

If we look at the three crystal structures in order (Bone et al., 1987; Matthews et al., 1975) and our present work, bearing in mind all the other experimental work cited, we conclude that the available evidence supports this proposed mechanism. In the structure of Bone et al. (1987), the catalytic serine O_γ is 1.7 Å from the boron atom and the geometry at the boron atom is refined to nearly trigonal geometry. We could interpret this as the first instance in which the serine is making the attack. In the structure of Matthews et al. (1975), the tetrahedral intermediate is reported. The hydroxyl group attached to the boron atom of the inhibitor has not yet extracted a proton from the catalytic imidazole N_ϵ. In the present structure, we postulate that the hydroxyl group has condensed with the proton from histidine, facilitating an incipient nucleophilic attack by His-57 on the boron atom and leading to an incomplete coordinate covalent B–N bond. To the extent that this interpretation is valid, we have captured and here report a time-averaged and space-averaged reaction intermediate in an enzyme.

From modeling considerations, a simple torsional rotation about the Ser C_β–O_γ bond should permit the close B–N contact necessary for formal bonding. However, a lever arm displacement of the Ile side chain would be involved, leading to rotation and translation and subsequent collision with the S_1 subsite of PPE. If so, a less bulky P_1 side chain (e.g., Ala) should favor this movement. Yet, Bone et al. (1989) report in their α-lytic protease studies that P_1 Ala and even Ile do not form a B–N coordinate covalent bond, only Phe does. Moreover, α-lytic protease stereochemically selects for L-allo-Ile, which, like the Met complex, is positioned rather "out" of the S_1pocket with C_γ–C_δ atoms pointing toward residue 192B of α-lytic protease. Only the P_1 Phe complex forms an apparent coordinate covalent bond. One also concludes that the S_1 pocket is deeper in PPE than in α-lytic protease, because in the α-lytic protease, no P_1 atom beyond the C_γ position points into the S_1 pocket but rather is found out of the pocket, parallel to Arg-192B of the α-lytic protease. Phe fits the S_1 pocket even more poorly, markedly displacing the inhibitor toward His-57. Collectively, in the absence of other information, the tentative conclusion is that the sterically displaced inhibitor, rather than the His-57, is the causative agent in this remarkably close (2.2 Å) contact, energetically mediated by numerous van der Waals attractions and repulsions, the formation and subsequent release of a molecule of water, and the electronic interactions of N and B atoms. Why, then, is this N–B bond not consummated? These crystallographic studies provide key pieces in a still incomplete puzzle.

The position of the P_1 C_α atom in this and other inhibitor complexes gives an indication of the translational latitude

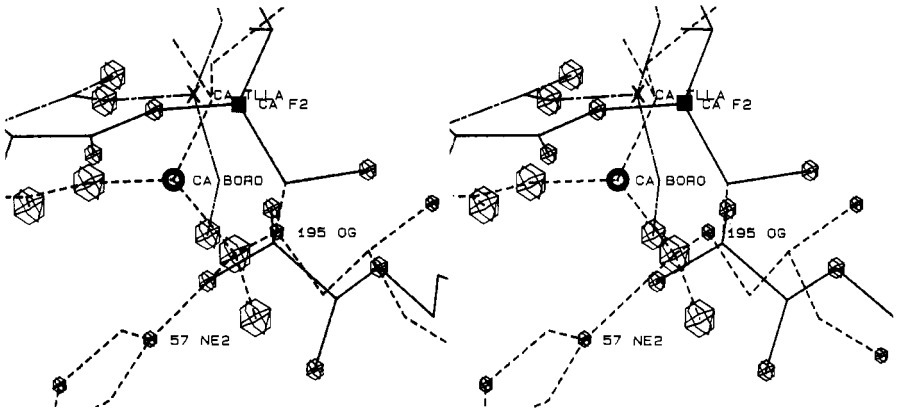

FIGURE 3: Trypsin plus leupeptin complex TLLA (Bode et al., unpublished results) drawn as dash-dot lines (the P_1 C_α atom is marked with ×) superimposed on the title complex (using the program ROTMOL; Radhakrishnan, unpublished program), which is drawn as dashed lines (the P_1 C_α atom is marked with O) (BORO). The peptidyl difluoromethyl ketone (F2) structure (Takahashi et al., 1989) is drawn as solid lines (the P_1 Val C_α atom is marked with ■). The relevent distances of P_1 C_α positions (×–■ = 1.2 Å; ×–O = 1.5 Å, ■–O = 1.8 Å) represent current upper limits of displacement into and out of the active site of superimposed serine proteases covalently bound by peptidyl inhibitors.

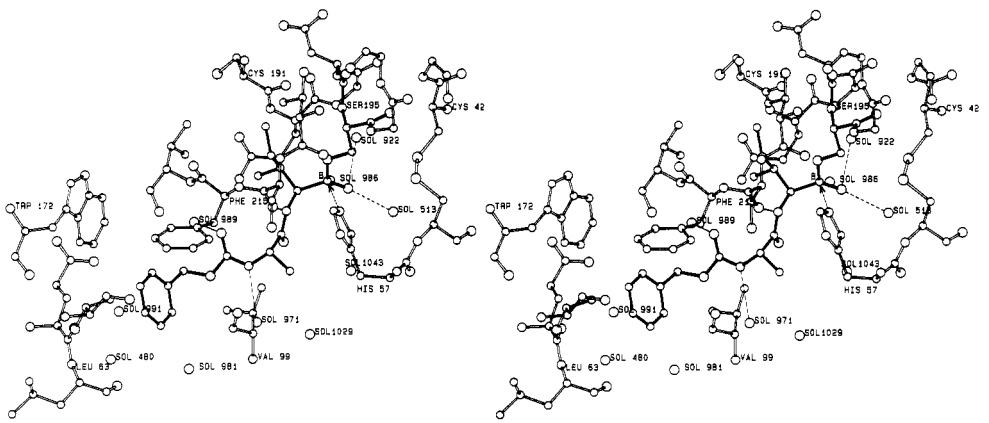

FIGURE 4: Binding of the ZAIB inhibitor to the active site of PPE drawn in stereo. H-bonds are shown with dashed lines; the N–B coordinate covalent approach is shown with an arrow. The water molecule (Sol-922) is shown in the oxyanion hole. The pictures were drawn by using a program written by one of the authors (Radhakrishnan, unpublished program).

exhibited by these serine proteases. For comparison TLLA (leupeptin: Ac-Leu-Leu-arginal plus trypsin; 1.5-Å resolution; Bode et al., unpublished results) and the peptidyl difluoromethyl ketone [Ala-Pro-Val-CF2-β-keto amide with PPE (Takahashi et al., 1989)] were superimposed onto the title complex by using the program ROTMOL (Radhakrishnan, unpublished program); the RMS deviations were 0.57 Å for 474 backbone atoms (NCCO) and 0.184 Å for 652 backbone atoms, respectively. In both cases, Ser-195 O_γ is covalently bonded to the P_1 carbonyl C atom; here it is bonded to the analogous B atom. The fluoromethyl ketone inhibitor has Val at the P_1 position, in comparison to Ile in the title complex. TLLA has Arg at P_1. The overlapping structures (Figure 3) show that the three C_α positions form a triangle. Both reference compounds are *deeply inserted* approximately equally into the S_1 pocket, and the P_1 C_α of the title complex is shifted 1.5 Å *out* of the S_1 pocket, away from the TLLA P_1 C_α position. It is striking that the isoleucine residue of ZAIB does not insert itself deeply into the S_1 pocket, and, in fact, Figure 3 shows that the C_β atom of the isoleucine residue is situated close to the C_α position of the valine residue in the difluoromethylketone inhibitor. These displacements are the largest thus far reported and indicate an approximate upper limit of the experimentally determined positional latitude permitted for complexes of serine proteases. Such a simple, one-dimensional metric should be factored into any mechanistic interpretation of proteolysis (Dutler & Bizzozero, 1989) and should prove useful in the design of novel inhibitors. The isoleucine residue does not fit well into the S_1 pocket, which in this case provides the geometry at the boron atom optimally oriented for attack by the histidine.

Currently, kinetic, NMR, and crystallographic studies on boronic acid inhibitors with α-lytic protease have also suggested the possibility of histidine acting as a nucleophile, and the mode of inhibition appears to be dependent on the amino acid residue at P_1 (Bachovchin et al., 1986; Farr-Jones et al., 1986). These authors report the adduct between boronic acids and Ser-195, which they call type 1 (good) substrates, and the boronic acids adducted to His-57 as type 2 (poor) substrates. They speculated that the initial binding was the formation of a ground-state complex, and the slower time-dependent kinetic stages involved the formation of a transition-state-like tetrahedral complex of boronic acid and active-site serine. They were able to distinguish between these two types of substrates by proton nuclear magnetic resonance and observed the boron atom of the inhibitor being attacked by His-57. Kettner and Shenvi reported a peptidyl boronic acid inhibitor of α-lytic protease (Bone et al., 1987) that had a phenylalanine residue in the P_1 position. The K_i for this inhibitor was 270 nM. Kettner and Shenvi (1984) have also noted that slow-binding inhibition was dependent on the residues at the primary specifity pocket of the enzyme. Our result, while agreeing with their results, also

offers an explanation for the molecular basis for such slow-binding inhibition, but does not address the time dependence of such a transition.

Another class of inhibitors, whose mechanism includes a nucleophilic histidine, are the chloromethyl ketones. First, serine attacks to give the tetrahedral intermediate, then His N_ϵ alkylates possibly via an epoxide intermediate. The structure of the enzyme–inhibitor complex contains two covalent bonds. As with the boronic acid inhibitors, the covalent bonding of the inhibitor to the enzyme is essential for histidine alkylation to occur. Interestingly, for the series of chloromethyl ketones tested (Powers et al., 1977) with the general formula Ac-Ala-Ala-Pro-X-CH_2Cl, the best inhibitor for PPE contained an isoleucine in P_1. This is in good agreement with the results presented here. Because the isoleucine residue cannot completely fit into the S_1 subsite of PPE, it presumably orients the reactive centers of the inhibitors for enhanced nucleophilic attack by His-57.

In the present structure, the boron hydroxyl oxygen atom is not located in the oxyanion hole (Robertus et al., 1972). Because the complex resembles the acyl enzyme (trigonal boron), it is reasonable to expect that one of the hydroxyl groups be located in the oxyanion hole upon binding to the enzyme. However, it is clear that the steric bulk of the isoleucine residue interacting with the active-site residues of the enzyme that form the S_1 pocket causes a marked displacement of the B atom away from the S_1 pocket, thus causing the hydroxyl group to be displaced from the oxyanion hole.

There is only one intermolecular hydrogen bond in the title complex (cf. Figure 2). The amido N atom of the Ile residue of the inhibitor makes a weak H-bond (3.0 Å) to the carbonyl oxygen atom of Ser-214. The carbonyl O atom of the carbobenzoxy group makes a poor contact (3.5 Å) to the amido nitrogen atom of Val-216. Contacts similar to these are also found in β-pleated sheet formations with other substrates and inhibitors. Although only two hydrogen bonds contribute to this arrangement here, the inhibitor binds in a productive antiparallel β-pleated sheet arrangement with the enzyme similar to other peptidic inhibitor complexes (Bode et al., 1989).

The phenyl group of the CBZ moiety is involved in an energetically favorable nonbonded interaction with Phe-215 of the enzyme's S_3 subsite (cf. Table II; Meyer et al., 1987). These aromatic–aromatic interactions, although contributing only ca. −10 kcal/mol to the energy of the complex, have been shown to play important roles in protein folding and stabilization (Burley & Petsko, 1985). The final refined structure of the inhibitor bound to the enzyme is shown in Figure 4.

This crystallographic result explains why the boronic acid inhibitor with isoleucine in the S_1 pocket (Figure 2) of PPE seems to be much a better inhibitor than the comparable ones with valine or alanine. In effect, the poor penetration of the isoleucine into the S_1 pocket has made possible an additional, favorable interaction between the His-57 N_ϵ and the boron atom. This displacement facilitates a nucleophilic attack by His-57 on the inhibitor. More studies with different residues at the primary specificity pocket, and preferably done at low temperatures, will be required to state unequivocally the mechanism of inhibition of the boronic acids to these serine proteases. The subsite geometric displacement reported here adds another data point to the description of productive active-site interactions of the serine proteinases. Such information is essential for understanding the intricacies of enzyme–ligand interactions at each step along the catalytic pathway, especially involving small peptide and heterocyclic substrates and inhibitors. It also offers new insights that may be useful for the design of drugs and mechanism-based inhibitors.

ACKNOWLEDGMENTS

We thank Dr. R. Bone for providing us with a copy of his initial manuscript. We acknowledge Professor R. Huber and Dr. W. Bode for providing experimental facilities, encouragement, and fruitful discussions. We thank Prof. John Katzenellenbogen at the University of Illinois for providing the inhibitor compound and Dr. John Dinkel, Associate Provost for Computing, for providing computational resources.

REFERENCES

Antonov, V. K., Ivanina, A. G., Berezin, I. V., & Martinek, K. (1970) *FEBS Lett. 7*, 23–25.

Bachovchin, W. W., Wong, W. Y. L., Farr-Jones, S., Kettner, C. A., & Shenvi, A. B. (1986) *Bull. Magn. Reson. 8*, 189–194.

Bachovchin, W. W., Wong, W. Y. L., Farr-Jones, S., Shenvi, A. B., & Kettner, C. A. (1988) *Biochemistry 27*, 7689–7697.

Berry, S. C., Fink, A. L., Shenvi, A. B., & Kettner, C. A. (1988) *Proteins: Struct. Funct. Genet. 4*, 205–210.

Bode, W., Wei, A.-Z., Huber, R., Meyer, E., Travis, J., & Neumann, S. (1986) *EMBO J. 5*, 2453–2458.

Bode, W., Meyer, E., Jr., & Powers, J. C. (1989) *Biochemistry 28*, 1951–1963.

Bone, R., Shenvi, H., Kettner, C. A., & Agarwal, P. A. (1987) *Biochemistry 26*, 7609–7614.

Bone, R., Frank, D., Kettner, C. A., & Agard, D. A. (1989) *Biochemistry* (preceding paper in this issue).

Bürgi, H. B., Dunitz, J. D., & Shefter, Eli (1973) *J. Am. Chem. Soc. 95*, 5065–5067.

Burley, S. K., & Petsko, G. A. (1985) *Science 229*, 23–28.

Deisenhofer, J., Remington, S. J., & Steigemann, W. (1985) *Methods Enzymol. 115B*, 303–323.

Dutler, H., & Bizzozero, A. S. (1989) *Acc. Chem. Res. 22*, 322–327.

Farr-Jones, S., Bachovchin, W. W., Kettner, C. A., & Shenvi, A. B. (1986) *Bull. Magn. Reson. 8*, 195.

Forsyth, J. B., & Wells, M. (1959) *Acta Crystallogr. 12*, 412–415.

Geneste, P., & Bender, M. L. (1969) *Proc. Natl. Acad. Sci. U.S.A. 64*, 683–685.

Harper, J. W., Cook, R. R., Roberts, C. J., McLaughlin, B. J., & Powers, J. C. (1984) *Biochemistry 23*, 2997–3002.

Jack, A., & Levitt, M. (1978) *Acta Crystallogr. 34A*, 931–935.

Kettner, C. A., & Shenvi, A. B. (1984) *J. Biol. Chem. 259*, 15106–15114.

Kinder, D. H., & Katzenellenbogen, J. A. (1985) *J. Med. Chem. 28*, 1917–1925.

Kraut, J. (1977) *Annu. Rev. Biochem. 46*, 331–358.

Lindquist, R. N., & Terry, L. (1974) *Arch. Biochem. Biophys. 160*, 135–144.

Luzatti, V. (1952) *Acta Crystallogr. 5*, 802–810.

Matthews, D. A., Alden, R. A., Birktoft, J. J., Freer, S. T., & Kraut, J. (1975) *J. Biol. Chem. 250*, 7120–7125.

Messerschmidt, A., & Pflugrath, J. W. (1987) *J. Appl. Crystallogr. 20*, 306–315.

Meyer, E. F., Jr., & Bode, W. (1987) in *QSAR in Drug Design and Toxicology* (Hadzi, D., & Jerman-Blazic, B., Eds.) pp 247–254, Elsevier, Amsterdam.

Meyer, E. F., Radhakrishnan, R., Cole, G. M., & Presta, L. G. (1986) *J. Mol. Biol. 189*, 533–539.

Meyer, E., Cole, G., Radhakrishnan, R., & Epp, O. (1987) *Acta Crystallogr. 44*, 26–38.
Moeckli, P., Schwarzenbach, D., Bürgi, H.-B., Hauser, J., & Delly, B. (1988) *Acta Crystallogr. B44*, 636–645.
Muetterties, E. L. (1967) *The Chemistry of Boron and Its Compounds*, Wiley, New York.
Nakatani, H., Hanai, K., Uehara, Y., & Hiromi, K. (1975a) *J. Biochem. 77*, 905–908.
Nakatani, H., Uehara, Y., & Hiromi, K. (1975b) *J. Biochem. 78*, 611–616.
Papamokos, E., Weber, E., Bode, W., Huber, R., Empie, M. W., Kato, T., & Laskowski, M. (1982) *J. Mol. Biol. 158*, 515–537.
Phillip, M., & Bender, M. L. (1971) *Proc. Natl. Acad. Sci. U.S.A. 68*, 478–480.
Powers, J. C., & Gupton, B. F. (1977) *Methods Enzymol. 46*, 208–216.
Powers, J. C., Gupton, B. F., Harley, A. D., Nashino, N., & Whitley, R. F. (1977) *Biochim. Biophys. Acta 485*, 156–166.
Robertus, J. D., Kraut, J., Alden, R. A., & Birktoft, J. (1972) *Biochemistry 11*, 4293–4303.
Robillard, G., & Schulman, R. G. (1974) *J. Mol. Biol. 86*, 519–540, 541–558.
Schechter, I., & Berger, A. (1967) *Biochem. Biophys. Res. Commun. 27*, 157–162.
Steigemann, W. (1974) Ph.D. Thesis, T.U. Munchen.
Stein, R. L. (1985) *J. Am. Chem. Soc. 107*, 5767–5775.
Swanson, S. M. (1988) *Acta Crystallogr. A44*, 437–442.
Takahashi, L. H., Radhakrishnan, R., Rosenfield, R. E., Meyer, E. F., Jr., Trainor, D. A., & Stein, M. (1988) *J. Mol. Biol. 201*, 423–428.
Takahashi, L. H., Radhakrishnan, R., Rosenfield, R. E., Meyer, E. F., Jr., & Trainor, D. A. (1989) *J. Am. Chem. Soc. 111*, 3368–3374.
Thompson, R. C., & Blout, E. R. (1973) *Biochemistry 12*, 51–57.
Travis, J., & Salvensen, G. S. (1983) *Annu. Rev. Biochem. 52*, 655–709.
Tsai, I., & Bender, M. L. (1984) *Arch. Biochem. Biophys. 228*, 555–559.
Zimmerman, M., & Ashe, B. M. (1977) *Biochim. Biophys. Acta 480*, 241–245.

Conformational Lability of Vitronectin: Induction of an Antigenic Change by α-Thrombin–Serpin Complexes and by Proteolytically Modified Thrombin†

Bianca R. Tomasini,‡,§ Maurice C. Owen,‖ John W. Fenton II,⊥ and Deane F. Mosher*,‡

Departments of Medicine and Physiological Chemistry, University of Wisconsin, 1300 University Avenue, Madison, Wisconsin 53706, Department of Pathology, The Christchurch School of Medicine, Christchurch, New Zealand, and Wadsworth Center for Laboratories and Research, New York State Department of Health, Albany, New York 12201

Received March 16, 1989; Revised Manuscript Received May 18, 1989

ABSTRACT: We previously showed that the α-thrombin–antithrombin III complex causes an antigenic change in vitronectin as monitored by the monoclonal anti-vitronectin antibody 8E6 (Tomasini & Mosher, 1988). We have extended these studies to other protease–serpin complexes and to γ-thrombin, a proteolytic derivative of α-thrombin. In the presence of heparin, recognition of vitronectin by 8E6 was increased 64- or 52-fold by interaction with the complex of α-thrombin and heparin cofactor II or the Pittsburgh mutant (Met_{358} → Arg) of α_1-proteinase inhibitor, respectively. This was comparable to the value obtained with the α-thrombin–antithrombin III complex. Factor Xa–serpin complexes were approximately 4-fold less effective than the corresponding thrombin complexes. α-Thrombin–serpin complexes but not Xa–serpin complexes formed disulfide-bonded complexes with vitronectin. Antigenic changes and disulfide-bonded complexes were not detected when trypsin- or chymotrypsin–serpin complexes were incubated with vitronectin. γ-Thrombin caused 7- and 34-fold increases in recognition of vitronectin by MaVN 8E6 in the absence and presence of heparin, respectively. In contrast, α-thrombin by itself had no effect. The antigenic change induced by γ-thrombin was maximal when γ-thrombin and vitronectin were equimolar, was not dependent on cleavage of vitronectin, and was abolished by inhibition of γ-thrombin with Phe-Pro-Arg-chloromethyl ketone but not with diisopropyl fluorophosphate. These data indicate that α-thrombin is the component in α-thrombin–serpin complexes that induces the antigenic change in vitronectin, probably via a region that is preferentially exposed in γ-thrombin.

Vitronectin is a plasma and serum glycoprotein that promotes cell–substratum adhesion (Hayman et al., 1985b; Silnutzer & Barnes, 1985). The binding of vitronectin to activated platelets (Thiagarajan & Kelly, 1988) and endothelial cells in suspension (Preissner et al., 1988) can be partially inhibited by peptides containing an Arg-Gly-Asp sequence, suggesting binding to the integrin receptors for vitronectin on these cells (Pytela et al., 1986; Suzuki et al., 1987). Vitronectin is also involved in the coagulation and complement systems. As S-protein (Jenne & Stanley, 1985; Preissner et al., 1986; Tomasini & Mosher, 1986), vitronectin incorporates into the membrane attack complex of complement, C5b-9, thus preventing binding of the attack complex to bystander cells not

† Supported by National Institutes of Health Grants HL13160 and HL29586.
* To whom correspondence should be addressed at the Department of Medicine, University of Wisconsin.
‡ University of Wisconsin.
§ Present address: La Jolla Cancer Research Foundation, 10901 N. Torrey Pines Rd, La Jolla, CA 92037.
‖ The Christchurch School of Medicine.
⊥ New York State Department of Health.

0006-2960/89/0428-7617$01.50/0